barriers decrease by 2.0 and 3.8 kcal/mol, respectively.

Concluding Remarks

Because of computational limitations we have been unable to introduce the effect of correlation energy and the effect of surrounding medium simultaneously. Nevertheless, we can make the approximation that corrections due to environmental effects and those due to energy correlation at the MP2 level are additive. In this case, the final values for the energy barriers in the Lipscomb mechanism with an additional water molecule turn out to be 10.8 kcal/mol (19.1 - 6.3 - 2.0) for the forward reaction and 3.7 kcal/mol (25.6 - 14.1 - 7.8) for the backward reaction. For the Lindskog mechanism the final value for the forward reaction turns out to be 6.0 kcal/mol (2.2 - 2.0 + 5.8), and for the backward reaction 6.9 kcal/mol (13.5 - 3.8 - 2.8). Thus, both mechanisms are acceptable to explain experimental data, because the values for their energy barriers are close to the maximum allowed value for this CO_2 hydration (ca. 10 kcal/mol).

The model used in the present work, because of computational constraints imposed by the size of the system studied, exhibits obvious limitations such as the level of calculation, the representation of the environment, and the lack of reoptimized geometries when including correlation energy or environmental effects. In any event, the main results of our work are to show that both mechanisms can be competitive in the CA enzymatic process, and that the study of the Lipscomb mechanism needs especially to have a precise modeling of the active site. Therefore, we conclude that, to get a definitive answer on the mechanism of CO_2 hydration catalyzed by the CA enzyme, it is necessary to follow these steps: first, to make a complete description of the active site and, second, to carry out a dynamical study where the coupling between the dynamics of the environment and that of the chemical system is well introduced, which requires that mutual electronic coupling is also well considered. Although this is not possible nowadays, it may be attained in the future.

Acknowledgment. This work has been supported by the Spanish "Dirección General de Investigación Científica y Técnica" under Project No. PB86-0529, and by the Commission of the European Communities (CEE) under Contract SC1.0037.C.

A Potential Surface Map of the H^-/HNO System. Relative Stabilities of NH_2O^- and ^-NHOH

John C. Sheldon* and John H. Bowie

Contribution from the Departments of Chemistry, The University of Adelaide, Adelaide 5001, South Australia, Australia. *Received May 20, 1991*

Abstract: The ion NH_2O^- has been observed in the gas phase, whereas its isomer ^-NHOH has not. The potential surface of the H^-/HNO system has been computed at the UMP2-FC/6-311++G**//RHF/6-31++G* level, and it shows three adducts, i.e. [H^-/HNO] (**1**), NH_2O^- (**2**), and ^-NHOH (**3**). Ion complex **1** is unstable with respect to **2**. Calculations [using the MP4(SDTQ)-FC-6-311++G**//HF/6-31++G** basis set] show that both NH_2O^- and ^-NHOH are strong bases [$\Delta H°_{acid}(NH_2OH)$ = 1629 and $\Delta H°_{acid}(NH_2OH)$ = 1669 kJ mol^{-1}] and that the electron affinities of the radicals $NH_2O^\bullet$ and $^\bullet NHOH$ are −1.2 and −16.7 kJ mol^{-1}, respectively.

Introduction

The nitroxide negative ion NH_2O^- is isoelectronic with the methoxide ion. It has been studied by molecular orbital theory,[1] but has been detected only twice. It may be formed by the reaction between hydroxylamine and HO^- (eq 1),[2] and in small yield by collision-induced dissociation of deprotonated amidoximes (e.g. eq 2).[3] Yet it is an elusive species since it cannot be prepared by the standard S_N2 (Si) reaction[4] from Me_3SiONH_2 (eq 3). Furthermore, its isomer ^-NHOH has not been observed, although it has been proposed that such a species is a powerful base, and that it may be stabilized as part of an ion complex (e.g. eq 4).[5]

$$NH_2OH + HO^- \rightarrow NH_2O^- + H_2O \quad (1)$$

$$Me(NH_2)C{=}NO^- \rightarrow [(MeCN)NH_2O^-] \rightarrow NH_2O^- + MeCN \quad (2)$$

$$NH_2^- + Me_3SiONH_2 \not\rightarrow NH_2O^- + Me_3SiNH_2 \quad (3)$$

$$MeCONOH \rightarrow {}^-CH_2CONHOH \rightarrow [(CH_2CO)^-NHOH] \rightarrow HC_2O^- + NH_2OH \quad (4)$$

We have explored the stability of NH_2O^- and ^-NHOH by the construction of the potential surface of the H^-/HNO system. This paper describes the construction of this surface and its major features. The two $\Delta H°_{acid}$ values of hydroxylamine are also calculated, together with the electron affinities of $NH_2O^\bullet$ and $^\bullet NHOH$.

Results and Discussion

The potential surface map for the reaction between the hydride ion and the HNO molecule is shown in Figure 1; the key features of this map are summarized in schematic form in Figure 2. The map shows three minima corresponding to [H^-(HNO)] (**1**),

(1) Magnussen, E. *Tetrahedron* **1985**, *41*, 5235. Magnussen, E. *J. Am. Chem. Soc.* **1984**, *106*, 1185. Hinde, A. L.; Pross, A.; Radom, L. *J. Comput. Chem.* **1980**, *1*, 118. Dewar, M. J. S.; Rzepa, H. S. *J. Am. Chem. Soc.* **1978**, *100*, 784.

(2) Lifshitz, C.; Ruttink, P. J. A.; Schaftenaar, G.; Terlouw, J. K. *Rapid Commun. Mass Spectrom.* **1987**, *1*, 61. J. K. Terlouw (personal communication) indicates that the ion was formed in the source of a ZAB 2F instrument from a mixture of $NH_2OH{\cdot}HCl$, finely powered NaOH, and H_2O in a glass vessel attached to the all quartz direct insertion probe (source pressure 5×10^{-4} Torr). The charge reversal (positive ion) spectrum shows the following relative intensities in the m/z 14–18 region: 14 (10), 15 (20), 16 (100), 17 (13), and 18 (2).

(3) Adams, G. W.; Bowie, J. H.; Hayes, R. N. *J. Chem. Soc., Perkin Trans. 2*, submitted for publication. The ion NH_2O^- is formed in low abundance: its collisional activation spectrum shows loss of $H^\bullet$, but the charge reversal spectrum shows peaks at [m/z (abundance)] 14 (<2), 15 (8), 16 (18), 17 (<2), 30 (100), 31 (25), and 32 (15). The major reaction of ion complex [$(MeCN)NH_2O^-$] (see eq 2) is formation of $^-CH_2CN$ and NH_2OH.

(4) DePuy, C. H.; Bierbaum, V. M.; Flippin, L. M.; Grabowski, J. J.; King, G. K.; Schmitt, R. J. *J. Am. Chem. Soc.* **1979**, *101*, 6443.

(5) Adams, G. W.; Bowie, J. H.; Hayes, R. N. *J. Chem. Soc., Perkin Trans. 2* **1991**, 689. Ion complex [$(CH_2CO)^-NHOH$] (eq 4) does not decompose to yield a detectable ion corresponding to ^-NHOH.

0002-7863/92/1514-877$03.00/0

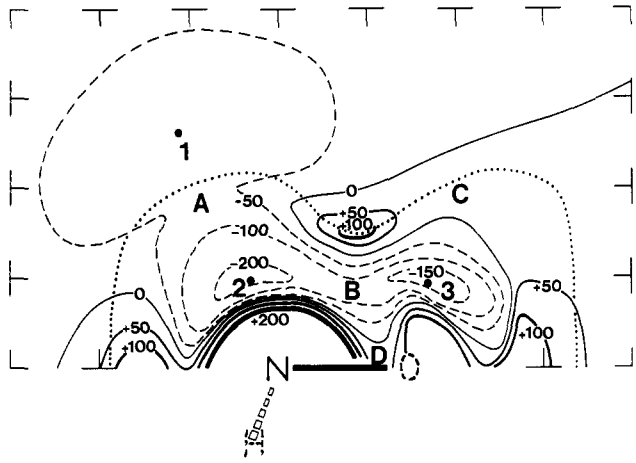

Figure 1. Potential surface map for the system H^-/HNO (UMP2-FC/6-311++G**//RHF 6-31++G*): (1) [H^-(HNO)]; (2) NH_2O^-; (3) $^-$NHOH. A, B, C, and D are saddle points for the following reactions: H^-(HNO) → NH_2O^-; NH_2O^- → $^-$NHOH; H^- + HNO → $^-$NHOH; and finally for an inversion where H passes between N and O. The dotted line on the map indicates the region where orientation of the H_2N bond direction changes rapidly from being coplanar with H_1 to being angled; i.e. above the dotted line hydrogen bonding may give a coplanar complex, e.g. complex **1**.

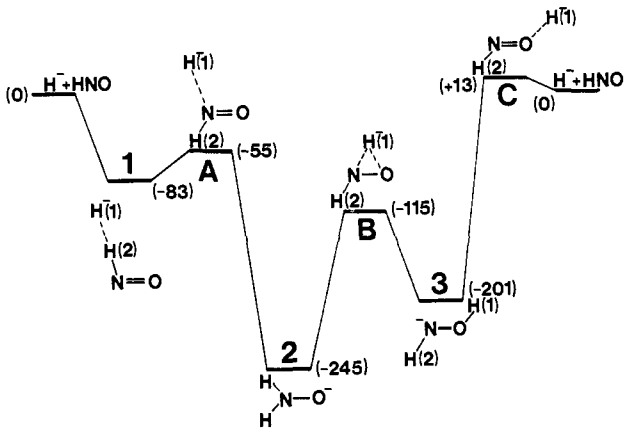

Figure 2. Conventional reaction coordinate diagram for the H^-/HNO system. Figures in parentheses are energies in kJ mol^{-1} relative to H^- + HNO (0 kJ mol^{-1}). Structural details for **2** and **3** are recorded in Table I. Other details are the following: (**1**) H_1H_2 1.48 Å, H_2N 1.05 Å, NO 1.19 Å, H_2NO, 108.9°; (**A**) H_1N 2.05 Å, NO 1.20 Å; (**B**) H_1N 1.26 Å, H_2N 1.01 Å, H_1O 1.10 Å, NO 1.54 Å; (**C**) H_2N 1.03 Å, NO 1.17 Å, H_1O 2.10 Å, H_2NO 108°, NOH_1 117°.

NH_2O^- (**2**), and $^-$NHOH (**3**) and it portrays the formation, interconversion, and reactions of these three species in a visually informative way. The molecular coordinates which undergo the major changes along these pathways are clearly those of hydride ion (H_1^-) as it moves around HNO. The system energy depends most strongly upon these two coordinates, namely (i) the distance of H_1 from nitrogen and (ii) the angle that H_1 makes to the NO bond. There remain four degrees of freedom (bond lengths and angles) which are notionally independent of the two H_1 coordinates already described. These are considered to be in equilibrium with the H_1^- location, since they will relax to such a state rather than remain random and unrelated. Thus we use the two dimensions of the map to display the two H_1 coordinates as the independent variables. The remaining coordinates cannot be shown on the map and are treated as dependent variables optimized for the location of H^-. The map is thus an arbitrary slice of the complete potential energy hypersurface, but one which provides the most chemically informative representation of the system under study.[6]

(6) A similar choice of coordinates has previously been made for the potential energy surface of the HNO molecule (i.e. the H/NO system), determined by spectroscopic procedures.[7]

Table I. Ab Initio Calculations for NH_2O^-, $^-$NHOH, $NH_2O^\cdot$, $^\cdot$NHOH, and NH_2OH[a,b]

	NH_2O^-		
	C_s symmetry; (i) −130.82268; (ii) 73.82		
NO	1.4069 Å	HNO	107.63°
NH	1.0119 Å	HNOH	110.36°
	HNOH		
	C_1 symmetry; (i) −130.80650; (ii) 69.90		
NO	1.4976 Å	HNO	99.60°
NH	1.0123 Å	HON	103.48°
HO	0.9373 Å	HNOH	106.90°
	$NH_2O^\cdot$		
	C_s symmetry; (i) −130.82420; (ii) 76.59		
NO	1.2661 Å	HNO	116.89°
NH	0.9983 Å	HNOH	147.96°
	$^\cdot$NHOH		
	C_s symmetry; (i) −130.81549; (ii) 76.85		
NO	1.3341 Å	HNO	102.44°
NH	1.0090 Å	HON	106.18°
HO	0.9425 Å		
	NH_2OH		
	C_s symmetry (trans staggered); (i) −131.44331; (ii) 116.13		
NO	1.3952 Å	H_1NO	105.66°
NH_1	1.0009 Å	H_2NO	105.66°
NH_2	1.0009 Å	HON	104.89°
HO	0.9401 Å	$HONH_1$	123.3°
		$HONH_2$	123.3°

[a] Geometries: UHF/6-311++G**//6-311++G** (radicals) and RHF/6-311++G**//6-311++G** for the anions and neutral hydroxylamine. Each geometry was tested for harmonic vibrational analysis to establish that it displayed only positive frequencies. Each molecular wave function was tested for stability, particularly on relaxing its spin multiplicity. [b] Energies: (i) MP4(SDTQ)-FC-6-311++G**//HF/6-311++G** (au) in hartrees, (ii) zero point vibrational energy [MP4(SDTQ)-FC-6-311++G**//HF/6-311++G**] in kJ mol^{-1}.

The map was constructed from 228 points, mostly within the shown 4 × 7 Å grid. The grid is oriented so that the lower edge lies along the NO bond direction, and the nitrogen atom remains fixed at a point on that edge. At each grid point, the non-hydride coordinates were optimized at the RHF/6-31++G* level (GAUSSIAN 86),[8] and the energy of this geometry partially corrected for electron correlation by second-order Möller–Plesset perturbation theory, i.e. at the MP2-FC/6-311++G*//RHF/6-31++G* level. The features of the map arise substantially from variational MP2 energies and are more reliably located than at the restricted Hartree–Fock level. The zero energy of the map refers to the isolated reactants, H^- and HNO.

The map shows three potential minima **1**, **2**, and **3** and a number of saddle points connecting them. If the H^- ion approaches the hydrogen of HNO (from the upper left of the map), it first forms the relatively weak hydrogen-bond complex [H^-(HNO)] (**1**), and there is no barrier to this process. Further progress of H_1 toward nitrogen results in the rearrangement of **1** to NH_2O^- (**2**) over saddle point **A**. In contrast, there is a barrier of 13 kJ mol^{-1} (saddlepoint **C**) when H^- approaches oxygen (from the upper right of the map) to form $^-$NHOH (**3**). The ions **2** and **3** may interconvert over saddle point **B**.

The map reveals two other points of interest. First, deprotonation of HNO by H^- to give dihydrogen and NO^- does not appear on the surface.[9] Second, saddle point **D** represents an

(7) Carter, S.; Dixon, R. N. *Mol. Phys.* **1985**, *55*, 701.

(8) Frisch, M. J.; Binkley, J. S.; Schlegel, H. B.; Raghavachari, K.; Melius, C. F.; Martin, R. L.; Steward, J. J. P.; Bobrowicz, F. W.; Rohlfing, C. M.; Khan, L. R.; Defrees, D. J.; Seeger, R.; Whiteside, R. A.; Fox, D. J.; Fleuder, E. M.; Pople, J. A. *Gaussian 86*; Carnegie-Mellon Quantum Chemistry Publishing Unit: Pittsburg, PA, 1984.

Table II. Calculated Electron Affinities of $NH_2O^•$ and $^•NHOH$ and Gas-Phase Acidities of NH_2OH [MP4(SDTQ)-FC/6-311++G**//RHF/6-311++G**][a]

EA, kJ mol^{-1}		$\Delta H°_{acid}$,[b] kJ mol^{-1}	
$NH_2O^•$	−1.2[c]	$NH_2O\underline{H}$	1629
$^•NHOH$	−16.7[d]	$N\underline{H}_2OH$	1669

[a] For individual geometries and energies see Table I. [b] $\Delta H°_{acid}(N\underline{H}_2OH)$ = (total energy H^+ + ^-NHOH + zero point energy correction) − (energy of NH_2OH + zero point energy correction) = (0.0 − 130.79025 + 0.02660) − (−131.44331 + 0.04420) = 0.63326 au = 1669 kJ mol^{-1}. Similarly, $\Delta H°_{acid}(NH_2O\underline{H})$ = (0.0 − 130.80685 + 0.02810) − (−131.44331 + 0.04420) = 0.62040 au = 1629 kJ mol^{-1}. [c] EA($NH_2O^- \rightarrow NH_2O^• + e$) = electronic energy difference (−4.0) + zero point energy difference (2.8) = −1.2 kJ mol^{-1}. The vertical transition energy from NH_2O^- to $NH_2O^•$ (at the geometry of the anion) is +41.5 kJ mol^{-1}. [d] EA($^-NHOH \rightarrow {}^•NHOH + e$) = electronic energy difference (−23.6) + zero point energy difference (6.9) = −16.7 kJ mol^{-1}. The vertical transition energy from ^-NHOH to $^•NHOH$ (at the geometry of the anion) is +39.2 kJ mol^{-1}.

unusual transit of H_1 between nitrogen and oxygen; these atoms are splayed to a separation of 2.3 Å at this point. Completion of this transit (out of the displayed grid) reforms **2** or **3** with changed orientation. The reported potential surface of HNO displays an entirely analogous feature: that potential surface is derived from empirical spectroscopic data.[7]

The potential map establishes that NH_2O^- and ^-NHOH are stable species at normal temperatures. The fact that these ions, particularly ^-NHOH, are difficult to detect experimentally does not then result from the bonding and structural features defined by the potential map. Thus we have calculated the electron affinities of the radicals $^•NHOH$ and $NH_2O^•$ from the data shown in Table I. In addition, since NH_2O^- and ^-NHOH are predicted to be powerful bases,[3,5] the two $\Delta H°_{acid}$ values of NH_2OH have also been calculated. Calculations were carried out at the MP4(SDTQ)-FC-6-311++G**//HF/6-311++G** level. The electron affinities and $\Delta H°_{acid}$ values are summarized in Table II. The data indicate that ^-NHOH is indeed a powerful base, since the $\Delta H°_{acid}$ value of its conjugate acid is 1669 kJ mol^{-1} [cf. $\Delta H°_{acid}(NH_3)$ = 1689 kJ mol^{-1} and $\Delta H°_{acid}(Me_2N\underline{H})$ = 1659 kJ mol^{-1}].[10] However, the electron affinity of $^•NHOH$ is appreciably negative (−16.7 kJ mol^{-1}), thus ^-NHOH should not be directly detectable since it is unstable with respect to its radical. The isomer NH_2O^- is also a strong base: the $\Delta H°_{acid}$ value of its conjugate acid is 1629 kJ mol^{-1} [cf. $\Delta H°_{acid}(H_2O)$ = 1635 kJ mol^{-1}].[11] In this case, the electron affinity of the radical $NH_2O^•$ is very close to zero (−1.2 kJ mol^{-1}); hence it is probable that both $NH_2O^•$ and NH_2O^- may be detectable,[12] although the lifetime of NH_2O^- is expected to be short. Hence theory and experiment are in accord for this system.

Acknowledgment. We thank the Australian Research Council for financial support.

Registry No. H^-, 12184-88-2; HNO, 14332-28-6; NH_2O^-, 51375-41-8; $NH_2O^•$, 13408-29-2; $^•NHOH$, 13940-32-4; NH_2OH, 7803-49-8.

(9) The potential surface deals with the optimized geometry of HNO with respect to H^-. There is no prior energization of HNO under these conditions and so the surface does not show a channel for elimination of dihydrogen. Instead, H^- moves to add to nitrogen (to ultimately form NH_2O^-). This movement causes disruption of the hydrogen bond and induces rotation of H_2 out of the plane of complex **1** to a dihedral angle schematically represented by the fragment shown in the center of the lower margin of Figure 1.

(10) MacKay, G. L.; Hemsworth, R. S.; Bohme, D. K. *Can. J. Chem.* **1976**, *54*, 1624.

(11) Schulz, P. A.; Mead, R. D.; Jones, P. L.; Lineberger, W. C. *J. Chem. Phys.* **1982**, *77*, 1153.

(12) In this context it is of interest that $NH_2O^•$ has been detected experimentally (Davies, P. B.; Dransfeld, P.; Temps, F.; Wagner, H. Gg. *J. Chem. Phys.* **1984**, *81*, 3763). In contrast, $^•NHOH$ has not been detected, and indeed it has been suggested that $^•NHOH$ may be thermodynamically unstable with respect to $NH_2O^•$.[2]

Computational Evidence for a Stable Intermediate in the Rearrangement of 1,2-$C_2B_4H_6$ to 1,6-$C_2B_4H_6$. A Second Try with a New Twist

Michael L. McKee

Contribution from the Department of Chemistry, Auburn University, Auburn, Alabama 36849.
Received July 15, 1991

Abstract: The rearrangement mechanism for the conversion of 1,2-$C_2B_4H_6$ to 1,6-$C_2B_4H_6$ was investigated by ab initio calculations. The reaction proceeds in two steps with a classical benzvalene-like intermediate. The first step, the rate-determining step, is a modified DSD (diamond–square–diamond) step where the symmetry of the transition state is reduced from C_{2v} to C_2 and thus changing the step from orbitally forbidden (in C_{2v} symmetry) to orbitally allowed (in C_2 symmetry). The second step is a concerted DSD step which is also known as a local bond rotation. The activation barrier is calculated to be 44.7 kcal/mol (MP4/6-31G*+ZPC//6-31G*), which is in good agreement with an experimental estimate (42–45 kcal/mol). A third calculated transition state provides a low-energy pathway for the interchange of two sets of equivalent borons in the intermediate.

Introduction

Sixteen years ago a communication with the above title appeared in this journal by Halgren, Pepperberg, and Lipscomb[1] (HPL), who noted that "few reaction pathways in rearrangements of boron compounds are well understood". Although progress has been made,[2-10] this statement is nearly as true today as it was then. The authors (HPL) used a synchronous-transit method[11] to de-

(1) Halgren, T. A.; Pepperberg, I. M.; Lipscomb, W. N. *J. Am. Chem. Soc.* **1975**, *97*, 1248.

(2) *Advances in Boron and the Boranes*; Liebman, J. F., Greenberg, A., Williams, R. E., Eds.; VCH: New York, 1988.

(3) *Electron Deficient Boron and Carbon Clusters*; Olah, G. A., Wade, K., Williams, R. E., Eds.; Wiley: New York, 1991.

(4) Gimarc, B. M.; Ott, J. J. *Inorg. Chem.* **1986**, *25*, 83.

(5) Wales, D. J.; Stone, A. J. *Inorg. Chem.* **1987**, *26*, 3845.

0002-7863/92/1514-879$03.00/0